32nd Electric Vehicle Symposium (EVS32)
Lyon, France, May 19 - 22, 2019

Viability of traction battery for battery-hybrid trolleybus

Abhishek Singh Tomar[1], Bram P.A. Veenhuizen[1], Lejo Buning[1], Ben Pyman[1]
[1]*HAN University of Applied Sciences, Ruitenberglaan 29, 6826 CC Arnhem, The Netherlands,AbhishekSingh.Tomar@han.nl*

Abstract

In the present work, a traction battery is proposed as a solution for extending the driving range of existing trolleybuses in the municipalities of Arnhem and Renkum (The Netherlands). It is mainly considered due to the possibility of in-motion charging (IMC) of the traction battery during the operation of trolleybus under the overhead grid network, which also eliminates the need for a separate charging infrastructure. The minimum requirements for the traction battery is established by determining the energy consumption of trolleybuses, which is derived from the measurements performed on different trolleybus lines. A simple Rint model of traction battery is developed using the manufacturer data of a LTO battery cell. Furthermore, three IMC strategies are developed and implemented using a battery management system for analysing the viability of proposed hybridization.

Keywords: energy consumption, public transport, battery electric vehicle, charging, battery management system.

1 Introduction

According to European Environmental Agency, approx. 19% greenhouse gas emissions in 2015 were contributed by heavy duty trucks and buses [1]. The clean and emission free public transportation is not only desirable for maintaining the health of cities and its occupants but also for achieving the climate goals (i.e. the reduction of greenhouse gas emissions by 80-95% by 2050 with respect to 1990 levels) of the Paris agreement. Trolleybuses are one of the noise free and energy efficient public transport solutions which use electricity from an overhead grid network and produce local zero emissions. At present, trolleybuses provide public transportation in more than 300 cities worldwide, which also include one or more cities in almost all of the European countries except Belgium, Croatia, Denmark and Finland.
In the Netherlands, the trolleybus cities are the municipalities of Arnhem and Renkum. One of the challenge faced by the trolleybus cities are the expansion of trolleybus route, which is typically limited by the extent of the overhead grid network. One pragmatic solution is to expand the grid network, which is both economically demanding and technically challenging by considering the infrastructure requirements. Another more intriguing solution is to convert the existing trolleybuses into battery-hybrid trolleybuses using a traction battery. The foremost advantage of this hybridization is the possibility of in-motion charging (IMC), which is potentially available when the trolleybus operates inside the grid network. A separate charging infrastructure may not be required due to the IMC but the feasibility strictly depends on the design/planning of the extended route for the battery-hybrid trolleybuses and the capacity of traction battery.
The battery-hybrid trolleybuses are not new and being operated in multiple European cities such as Castell*ó*n, Cagliari, Eberswalde, Esslingen, Gdynia, Geneva, Rome, Solingen, Szeged, etc. More European cities such as Lublin, Prague, Pilsen, Rimini, Salzburg etc. are on their way to implement and test this hybrid concept. However, the hybrid solution (i.e. traction battery capacity + route extension + charging strategy) which is practical and feasible in one city, may or may not be practical in another city. It may be comprehended by considering the following points:

- no two cities are same by considering their climate, topography and number of passengers using the trolleybuses;
- the trolleybuses (i.e. electric motor, number of drive axles, climate control unit, etc.) may be different depending on the respective manufacturer and component supplier;
- the nominal and maximum specification of the overhead grid (i.e. current, voltage and impedence) may also be different.

In other words, next to operational conditions and driver influences, the energy consumption of the trolleybus is specific to the city. Additionally, the desired driving range extension and respective overhead grid network specifications need to be considered to design the traction battery and IMC strategy, and thus feasibility of this hybridization.
This paper presents such an approach for the city of Arnhem, where the energy consumption of the existing trolleybuses are determined using the real-world data measured during the normal operating conditions. Next, the minimum requirements for the traction battery is determined by considering a desired driving range extension of 10 [km]. Next, a suitable battery chemistry is selected based on the comparison of various commercially available lithium ion batteries. Next, a simplified Rint model of the traction battery is developed using the available manufacturer data of selected battery cell. Next, the viability of the hybridization is demonstrated with different IMC strategies. Finally, the assumptions and simplifications of the present work together with their implications are discussed.

2 Energy consumption of trolleybus

There are currently six trolleybus lines (Line 1, 2, 3, 5, 6 and 7) operated in the city of Arnhem. The measurements are performed on all the six trolleybus lines at certain times and days (according to the schedule provided by the trolleybus operator) in the month of December 2018 and January 2019 during their normal operation. The respective data is collected using the diagnostic system of the electrical component supplier (viz. Kiepe Electric GmbH) of the trolleybus. An overview of the collected data is presented in Table 1 with respect to the trolleybus line, respective source and destination, number of trips measured and approx. length of one single trip.

Table 1: Overview of the measured data

Line No.	Source to destination	No. of trips	Length of one trip [km]
1	Velp to Oosterbeek	11	11.5
1	Oosterbeek to Velp	12	11.5
2	Arnhem Central to De Laar West	10	8.5
2	De Laar West to Arnhem Central	11	8.3
3	Het Duifje to Burger Zoo	8	9.8
3	Burger Zoo to Het Duifje	11	10.3
5	Presikhaaf to De Zeis	8	14
5	De Zeis to Presikhaaf	8	14
6	De Laar West to HAN	7	12
6	HAN to De Laar West	7	11.5
7	Rijkerswoerd to Geitenkamp	8	12.6
7	Geitenkamp to Rijkerswoerd	8	12.6

The electric motor and climate control unit are the two main sources of energy consumption in existing trolleybuses. Electric motor requires energy to meet the propulsion demand of trolleybus and climate control unit requires energy to maintain the comfort temperature inside the trolleybus. Other than these two, approx. 3-5% energy is also required for compressed air controlled subsystems and miscellaneous functionalities of the trolleybus, such as lighting, dashboard, infotainment, etc. Since, it is very small compared to both electric motor and climate control unit, therefore, it has not been discussed explicitly but have been considered inclusive in the energy consumption of electric motor.

2.1 Climate control unit

The climate control unit requires energy to maintain thermal comfort of passengers inside the cabin. It operates an air-conditioning unit in summer, which removes the heat from the cabin and subsequently, reduce the cabin temperature compared to ambient (i.e. outside the cabin) temperature. During winter, it operates a heating unit, which adds the heat into the cabin and subsequently, increase the cabin temperature compared to ambient temperature. According to study conducted on trolleybuses [2], energy

consumption due to climate control unit may reach approx. 35% in summer and approx. 43% in winter with respect to the total energy consumption of trolleybus.
The heat balance method described by ASHRAE handbook HVAC applications [3] is a good method to analyse the factors affecting the energy consumption of climate control unit. The method considers the various phenomena which either add or remove the heat from the cabin and the resultant heat imbalance has to be negated by the climate control unit while considering the desired comfort temperature and thus, consuming energy. The net heat balance $\dot{Q}_{net}$ and subsequently, required electrical energy for climate control unit E_{cl} in [kWh] during winter may be described as presented in Equation 1 and 2, respectively. COP_h is the coefficient of performance of climate control unit with respect to heating.

$$\dot{Q}_{net} = U \cdot A \cdot (\dot{T}_{amb} - \dot{T}_{cab}) + \dot{m}_{fair} \cdot (e_{amb} - e_{cab}) + \dot{m}_{dair} \cdot (e_{amb} - e_{cab}) \cdot n_{do} + n_p \cdot \dot{Q}_p \quad (1)$$

$$E_{cl} = \frac{1}{3600} \int_0^t \left(\frac{\dot{Q}_{net}}{COP_h} \right) dt \quad (2)$$

The first term in the Equation 1 represents the conductive heat losses through the vehicle body (glass, metal and fibre), which may be determined using the overall heat transfer coefficient U of the vehicle body material, respective surface area A of the vehicle body material and rate of change of ambient $\dot{T}_{amb}$ and cabin temperature $\dot{T}_{cab}$. The second term in the Equation 1 represents the heat losses due to the fresh air circulation, which is required to maintain the air quality inside the cabin. It may be determined using mass flow rate of fresh air $\dot{m}_{fair}$ and enthalpies of ambient e_{amb} and cabin air e_{cab}. The third term in the Equation 1 represents the momentary heat losses due to the door opening at the bus stops, which may be determined using mass flow rate through the door opening $\dot{m}_{dair}$, number of doors opened at the bus stop n_{do} and enthalpies of ambient and cabin air. The forth term in the Equation 1 represents the metabolic heat gain due to the number of passengers inside the cabin. It may be determined using number of passengers inside the cabin n_p and the heat generated by one passenger $\dot{Q}_p$, which depends on the physical movement. Additionally, by considering the heat gain due to solar radiation in the Equation 1 and respective COP in Equation 2, the energy consumption of climate control unit with respect to air-conditioning may also be determined using the similar approach.

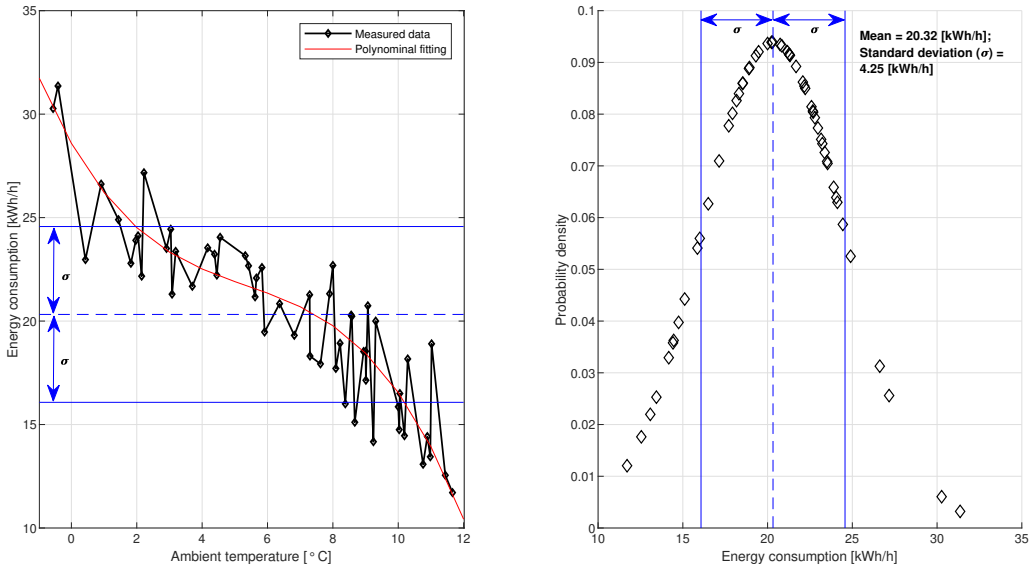

Figure 1: Energy consumption of the climate control unit for the trips measured on all trolleybus lines and normal distribution

It may be observed from the Equation 1 that the energy required for the climate control unit mainly depends on the factors such as ambient temperature, time duration of the trip, number of passengers, number of stops, etc. Another aspect to consider is that the energy consumption of the climate control unit is a time dependent quantity. In other words, if more time is taken to travel the same distance while keeping the other influencing factors same then more energy may be consumed by the climate control

unit. However, all of the influencing factors except the ambient temperature are trip specific and are also related to each other. Therefore, only ambient temperature can be explicitly correlated to the energy consumption of the climate control unit irrespective of the trolleybus line and the respective trips. Fig. 1 presents the energy consumption in [kWh/h] of climate control unit for all the measured trips with respect to their ambient temperature. It may be observed that with the decrease in the ambient temperature, the energy consumption increases irrespective of trolleybus line. The other trip related factors may be the cause of the observed variations. This correlation as presented in Fig. 1 may also be described using a 3rd degree polynominal expression with $RMSE = 1.898$ and $R^2 = 0.812$ as presented in Equation (3), where $\dot{E_{cl}}$ is the energy consumption of climate control unit in [kWh/h] and T_{amb} is the ambient temperature in $[^{\circ}C]$. It may be used as an initial prediction of energy consumption of climate control unit at the respective ambient temperature for battery management system.

$$\dot{E_{cl}} = -0.0256 \cdot T_{amb}^3 + 0.415 \cdot T_{amb}^2 - 2.764 \cdot T_{amb} + 28.59 \tag{3}$$

To determine the energy requirement for traction battery related to climate control unit, probability density of energy consumption is calculated for all the measured trips, which is schematically presented in Fig. 1. The mean value is 20.32 [kWh/h] with standard deviation of 4.25 [kWh/h]. Approx. 75 [%] of the measured trips are within 1 standard deviation from the mean value. The minimum energy required for traction battery with regard to the climate control unit $E_{cl_{bat}}$ may be calculated using Equation 4, where $\dot{E_{clmean}}$ is the mean of energy consumption as determined using the normal distribution, σ is the standard deviation and t_{mean} is the mean of time durations of all the measured trolleybus line trips lying within the 1 standard deviation region from the mean, which is approx. 0.57 [h].

$$E_{cl_{bat}} = (\dot{E_{clmean}} + \sigma) \cdot t_{mean} \approx 14 \ [kWh] \tag{4}$$

2.2 Electric motor

The electric motor in trolleybus consumes electrical energy and provide the mechanical energy at the wheels, which is required for the trolleybus movement while overcoming the various resistances. The required mechanical power at the wheels P_{mech} as described in [4] and subsequently, required electrical energy for the electric motor E_{EM} in [kWh] may be determined using Equation 5 and 6, respectively. η_{gb} is the efficiency of gearbox and η_{EM} is the efficiency of electric motor.

$$P_{mech} = (m + m_r) \cdot a \cdot v + \frac{1}{2} \cdot \rho_a \cdot A \cdot C_d \cdot v^3 + m \cdot g \cdot f_r \cdot \cos\theta \cdot v + m \cdot g \cdot \sin\theta \cdot v) \tag{5}$$

$$E_{EM} = \frac{1}{3600} \int_0^t \left(\frac{P_{mech}}{\eta_{gb} \cdot \eta_{EM}} \right) dt \tag{6}$$

The first term in the Equation 5 represents the mechanical power required to accelerate the trolleybus including its passengers and to overcome the rotational inertia. It may be determined using trolleybus mass including passengers m, mass representing rotational inertia m_r, trolleybus acceleration a and trolleybus velocity v. The second term in the Equation 5 represents the mechanical power required to overcome aerodynamic resistance, which may be determined using air density ρ_a, trolleybus front cross-sectional area A, air drag coefficient C_d and trolleybus velocity. The third term in the Equation 5 represents the mechanical power required to overcome rolling resistance, which may be determined using trolleybus mass, gravitational acceleration g, rolling resistance coefficient f_r, road gradient angle θ and trolleybus velocity. The forth term in the Equation 5 represents the mechanical power required to overcome gradient resistance, which may be determined using trolleybus mass, gravitational acceleration, road gradient angle and trolleybus velocity.
The gearbox efficiency, rotational inertia, front cross-sectional area and drag coefficient may be considered same for all the trolleybuses due to the fact that they are being supplied by the same manufacturer. The rolling resistance is also considered as constant by assuming the same brand of tires. With this consideration, the main variables, which influence the energy consumption of the electric motor are the electric motor efficiency, number of passengers (influencing the trolleybus mass), acceleration, velocity and road gradient angle. It may be comprehended that all of the influencing variables except the road gradient angle are trip dependent quantities, due to which the electric motor may consume different energy during the different trips on the same trolleybus line. However, the road gradient angle is the property of trolleybus line, which directly relates to the potential energy related to the trolleybus line. In other words, more energy will be consumed by electric motor during up-hill trip compared to the down-hill trip while considering the same trip dependent variables.
To compare the trolleybus lines, the energy consumption of electric motor in [kWh/km] is determined for all the measured trips and presented in Fig. 2. The difference in energy consumption during the trips on same trolleybus line between the same source and destination may be explained using the trip dependent variables. The energy consumption of electric motor on trolleybus lines 2 (red color), 5 (magenta color) and 6 (green color) may be considered similar during the respective round trips as the difference in mean

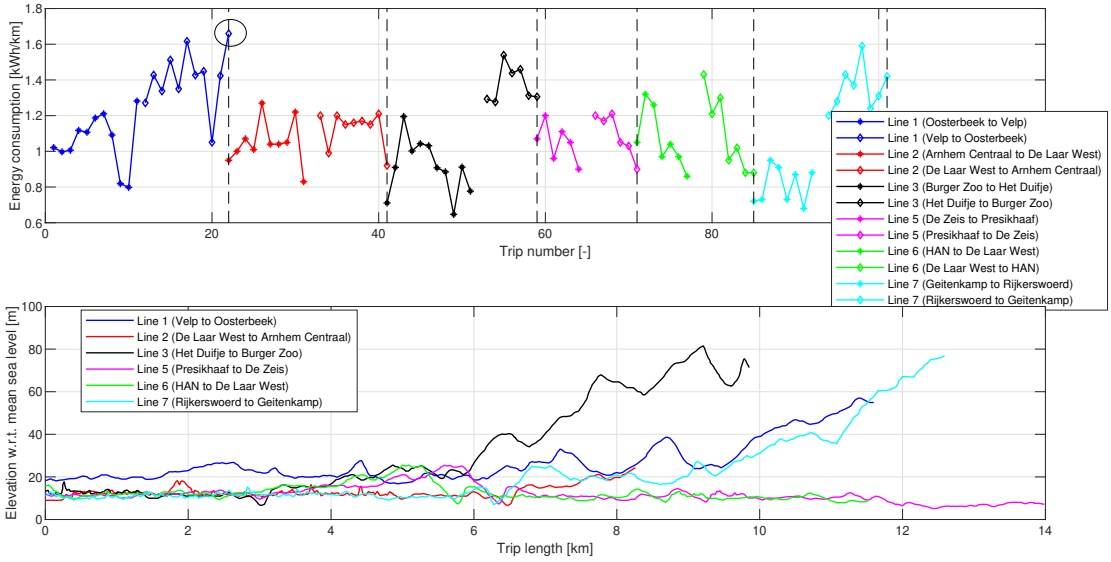

Figure 2: Energy consumption of electric motor for all the trolleybus lines and elevation profiles of respective trolleybus line

energy consumption between the round trips are approx. 0.08, 0.04 and 0.03 [kWh/km], respectively. It may also be comprehended from their respective elevation profiles presented in Fig. 2. On the contrary, the difference in mean energy consumption between the round trips of trolleybus lines 1 (blue color), 3 (black color) and 7 (cyan color) are approx. 0.35, 0.46 and 0.55 [kWh/km], respectively, which may also be comprehended from their respective elevation profiles. The trolleybus line 7 has the highest potential difference, followed by line 3 and then line 1, similar trends may also be observed from the difference in mean energy consumption between the round trips.
The maximum energy consumption of electric motor among all of the measured trolleybus line trips is considered to determine the energy requirement for traction battery related to electric motor, which is approx. 1.66 [kWh/km] corresponding to trolleybus line 1 (Velp to Oosterbeek) trip 22, encircled in Fig. 2.

3 Traction battery

The performance of battery-hybrid trolleybus in battery mode will directly depend on the capability of the traction battery. Therefore, it is critical to establish minimum requirements for the traction battery which are nothing but the minimum required performance characteristics of the traction battery in order to make this hybridization feasible and practical. The minimum performance characteristics, which needs to be established are the energy capacity, nominal voltage, current (or coulometric) capacity, charge and discharge C-rates. These minimum requirements may be determined using the existing trolleybuses and desired driving range extension, which is considered as 10 [km].
The minimum energy capacity required for the traction battery $E_{bat_{min}}$ can be determined using Equation 7, where $E_{cl_{bat}}$, is the traction battery energy required for the climate control unit as determined in Equation 4, $\frac{E_{EM}}{\Delta x}$ is the energy consumption of electric motor corresponding to the trolleybus line 1 (Velp to Oosterbeek) trip 22 determined as 1.66 [kWh/km] and x_{min} is the desired driving range.

$$E_{bat_{min}} = E_{cl_{bat}} + \frac{E_{EM}}{\Delta x} \cdot x_{min} \approx 30.6 \ \ [kWh] \tag{7}$$

The nominal voltage of the traction battery $V_{bat_{nom}}$ is determined by taking the average of overhead grid voltage during the trolleybus line 1 (Velp to Oosterbeek) trip 22, which is approx. 660 [V]. The current capacity of the traction battery $C_{bat_{min}}$ may be determined using Equation 8.

$$C_{bat_{min}} = \frac{E_{bat_{min}}}{V_{bat_{nom}}} \approx 46 \ \ [Ah] \tag{8}$$

The power demand of trolleybus is highly dynamic in nature which is mainly depicted by the current. It may also be represented by C-rate, which is a dimensionless quantity and may be determined using Equation 9, where I is the charge or discharge current.

$$Crate = \frac{I}{C_{bat_{min}}} \ [-] \tag{9}$$

The discharge and charge rates are determined using Equation 9 for the trolleybus line 1 (Velp to Oosterbeek) trip 22 and summarized in Table 2 by considering C-rate intervals. The negative C-rate represents the recuperation (or charging of traction battery) during braking and positive C-rate represents the discharging of the traction battery. The duration represent that the C-rate determined during the entire trip is found in the respective C-rate interval for the respective duration which is calculated cumulatively. The relative percentage is determined separately for both charging and discharging C-rates to represent the occurrence of respective C-rate interval during the trip.

Table 2: C-rate intervals and their cumulative duration in the trolleybus line 1 (Velp to Oosterbeek) trip 22

C-rate interval [-]	Current interval [A]	Duration [s]	Relative percentage [%]
-6.7 to -3.5	-309 to -161.4	42	19
-3.5 to 0	-161.4 to 0	181	81
0 to 3.5	0 to 161.4	1206	72
3.5 to 10.5	161.4 to 484.2	438	26
10.5 to 12.5	484.2 to 574.5	34	2

It may be observed that the majority of time C-rate lies within 3.5 during both charging and discharging, depicted by respective relative percentage in Table 2, therefore, nominal C-rate for the traction battery may be considered as 3.5 during both charging and discharging by considering the current capacity of 46 [Ah]. The traction battery must also be capable of C-rates greater than 10 and 3.5 during discharging and charging, respectively by considering the current capacity of 46 [Ah]. It may also be comprehended from the Equation 8 that the required C-rates will decrease with the the increase in current capacity.

3.1 Battery chemistry

It is important to select a suitable battery chemistry for the traction battery because the performance characteristics of a battery are dependent on its chemistry. Lithium ion batteries are one of the most preferred choice for electric vehicles due to their advantages over the other chemistries, such as high cell voltage, high power density, high energy density, high charge/discharge rate, etc. An intuitive way of characterising the lithium ion batteries is based on their cathode and anode material [5].

3.1.1 Cathode material

The cathode materials which are often available in commercial lithium ion batteries, are lithium cobalt oxide (LCO), lithium manganese oxide (LMO), lithium nickel manganese cobalt oxide (NMC), lithium iron phosphate (LFP) and lithium nickel cobalt aluminium oxide (NCA), etc. The current capacity and voltage of the cell depend on the crystal structure (such as layered, spinel, olivine and tavorite) of the cathode material [5]. The different cathode materials have their own advantages and disadvantages which make them suitable for specific application. For example, LCO batteries have advantage in terms of high energy density, high cell voltage and low self-discharge but also have disadvantage in terms of low thermal stability, fast capacity fade at high discharge rates and high cost due to cobalt. LMO batteries have higher power density, higher cell voltage and relatively low cost compared to LCO but their cyclic performance is worse because the crystal structure of LMO has a tendency to change during lithium ion extraction and also their calender life is limited due to the dissolution of manganese into electrolyte, which gets worse with the increasing operating temperature. NMC and NCA batteries in general are better than LCO batteries due to their higher energy density, higher thermal stability, low cost, higher life cycle. NCA batteries have higher energy density compared to NMC batteries but are comparatively less safe due to their lower thermal runaway temperature and have lower life cycle than NMC batteries. LFP batteries have lower energy and power density in comparison with the other lithium ion batteries but their discharge curve is flat and are most thermally stable.

3.1.2 Anode material

The above comparison is based on the lithium ion batteries with graphite (C) as the anode, which is most commonly used anode material. This is mainly due to its low cost, abundant availability, moderate

energy and power density and cycle life. Lithium titanium oxide (LTO) is another commercially available anode material and has superior thermal stability compared to graphite. The higher thermal stability of LTO is discussed in [6] using a open-circuit energy diagram of three lithium ion batteries (LCO/C, LNM/C and LFP/LTO). In simple words, the higher thermal stability is primarily due to the absence of solid electrolyte interface (SEI) layer in LTO batteries due to its lower Fermi level energy compared to graphite. However, the SEI layer is formed due to the reaction between the metal ions and electrolyte which may also occur in LTO batteries under certain conditions. In case of the presence of SEI layer, the thermal stability of the cell depends on the mechanical stability of the SEI layer. The another phenomenon which prevents the damage of SEI layer in the LTO batteries is the volumetric expansion of anode during the insertion of lithiun ions, which is negligible for LTO compared to graphite. The LTO based batteries have lower cell voltage, lower energy density and higher cost compared to graphite based batteries but they have significant advantages in terms of higher thermal stability, higher power density, higher charge and discharge rates and higher cycle life compared to graphite based batteries.

Table 3: Comparison of commercially available lithium ion batteries: '+' = better, '-' = worse and '.' = neutral performance of the battery with respect to LCO/C battery [5] - [12]

Characteristics	LMO/C	NMC/C	NCA/C	LFP/C	*/LTO
Cell voltage	+	+	-	- -	- - -
Energy density	-	+	++	- -	- - -
Power density	++	++	+++	+	++
C-rate	.	.	.	+	++
Thermal stability	-	+	+	++	+++
Safety	++	+	.	+++	+++
Life span	-	+	.	++	+++
Cost	++	+	+	+++	-

Table 3 presents a generic relative comparison between the commercially available lithium ion batteries with respect to the LCO/C battery. The batteries are designed to improve the specific characteristics according to the application. For example, the energy density and cell voltage of LTO based batteries can be significantly improved with the cathode material. It was shown by Ariyoshi et. al. [12], in which four LTO based cells using LFP, lithium aluminium manganese oxide (LAMO), NMC and lithium nickel manganese oxide (LNM) as cathode materials are compared. The cell voltages were found as 2.0, 2.5, 2.5 and 3.2 [V], respectively and the respective energy densities were found as 165, 165, 215 and 245 [Wh/kg], respectively. The trolleybus is a high power demanding application and based on the comparison presented in Table 3, LTO based batteries appear to be the best suitable option, especially by considering power density, C-rates, thermal stability, safety and life span.

3.2 Battery model

There are various approaches available in literature with regard to the battery modelling, such as mathematical models, electrochemical models and equivalent circuit models (ECMs). ECMs are the most widely used battery models for automotive applications due to their lower computation time and cost, good accuracy and less number of parameters. An ECM is modelled using resistors, capacitors and voltage sources to form an electrical circuit network. The Rint model is the simplest ECM, consisting an ideal voltage source representing open-circuit voltage and a resistor representing internal resistance of the battery, which is also known as 0RC model. To capture the dynamic response of the battery one or more parallel resistor-capacitor sub-circuits are added to the Rint model and are generally referred as nRC model (e.g. Thevenin model is 1RC ECM, Dual polarization model is 2RC ECM, etc.). In addition to the RC branches, one-state hysteresis can also be found in some ECM model. Theoretically, higher number of RC branches should correspond with the higher accuracy of the model but it also increases the complexity of the model and may lead to large errors in parameter identification and subsequently, leading to poor accuracies. It is concluded in the comparative studies [14] - [19], that 2RC ECM is both accurate and simple for automotive applications. However, it is necessary to perform the measurements on the LTO cell in order to identify the 2RC ECM parameters, which is not feasible in the scope of present work, therefore, Rint model is developed and used for the further analysis. The battery model is developed using the similar approach described in [18] while considering the following points:

- the open-circuit voltage (OCV) and internal resistance during charging and discharging vary with respect to the state of charge (SOC) of battery;
- the input to the model is power instead of current. The required current is calculated using the power and terminal voltage of the battery;
- a battery management system which monitors the battery cut-off voltage during both charging and discharging, C-rates, SOC and controls the charging power according to the IMC strategy.

A LTO cell from Altair [20] is used to parameterize the battery model, whose characteristics are presented in Table 4 and the respective OCV and internal resistance of the cell with respect to SOC is presented in Fig. 3.

Table 4: Characteristics of the 60 Ah Altair LTO cell [20]

Characteristics	Value
Nominal voltage	2.26 [V]
Discharge cut-off voltage at -40°C to 30°C	1.5 [V]
Discharge cut-off voltage at 30°C to 55°C	1.8 [V]
Charge cut-off voltage at -40°C to 20°C	2.9 [V]
Charge cut-off voltage at 20°C to 55°C	2.8 [V]
Maximum continuous charge/discharge current	360 [A]
10 [s] pulse charge/discharge current	600 [A]
Internal charge impedance (10 [s] DC pulse 50% SOC at 25°C)	0.38 [$m\Omega$]
Internal discharge impedance (10 [s] DC pulse 50% SOC at 25°C)	0.4 [$m\Omega$]
Internal impedance (1 [Hz] AC pulse 10% SOC at 25°C)	0.6 [$m\Omega$]
High rate current capacity (6C rate at 25°C)	60 [Ah]
High rate energy (6C rate at 25°C)	135.6 [Wh]
Specific power	1.33 [W/kg]
Specific energy	77 [Wh/kg]
Cycle life (2C charge and 2C discharge, 100% DOD at 25°C)	>16000
Cycle life (2C charge and 2C discharge, 100% DOD at 55°C)	>4000
Calender life at 25°C	>25 years

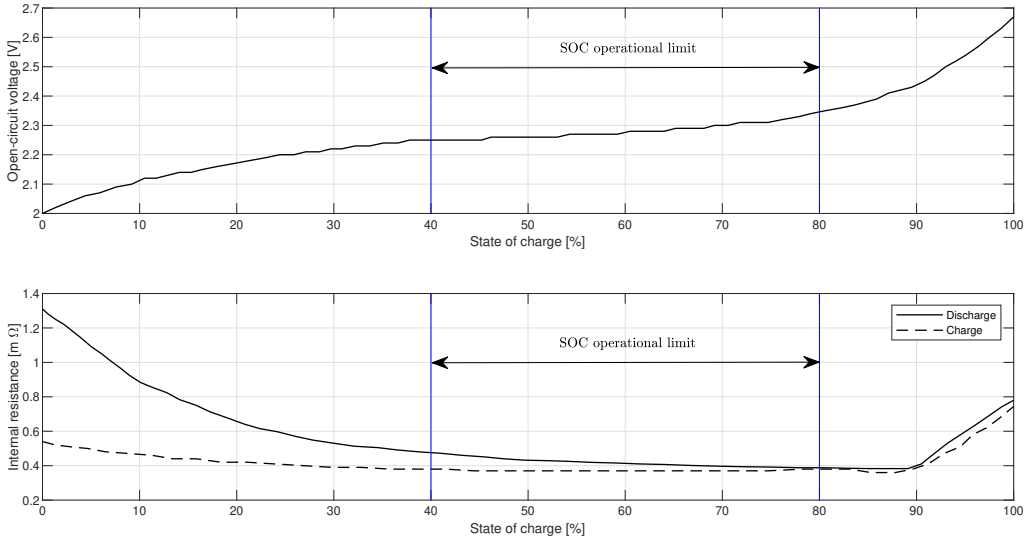

Figure 3: OCV and internal resistance characteristics of the 60 Ah Altair LTO cell

It may be observed from the Fig. 3 that the internal resistance of the cell during charging increases above 90% SOC and below 20% SOC in comparison with 20 to 90% SOC. The internal resistance during discharging is minimum between 80 to 90% SOC and increases with both increase in SOC above 90% and decrease in SOC below 80%. The high internal resistance will lead to high resistive loss during both charging and discharging which in turn will decrease the overall efficiency. Ideally, operation of traction battery between 50 to 90% SOC would be the best by considering its internal resistance. But in order to avoid the SOC increasing above 90%, which may occur due to the regeneration while the battery is at its upper SOC limit, an operational limit of 40 and 80 % is considered for SOC. A similar operational limit of 30-70% SOC may also be established based on the internal resistance of LTO cell presented in [21], which was measured during hybrid power pulse capability (HPPC) test with charging and discharging rates varying from 4 to 20.

It may be comprehended that by considering this operational limit, only 40% of the rated capacity of the traction battery will be usable, which must fulfil the minimum requirement of the trolleybus. Therefore, the rated energy capacity E_{bat} of the traction battery may be determined using Equation 10. Subsequently, number of cells in series $n_{s,bat}$ and parallel $n_{p,bat}$ may be determined using Equation 11 and 12, respectively.

$$E_{bat} = \frac{E_{bat_{min}}}{0.4} \approx 76 \ [kWh] \tag{10}$$

$$n_{s,bat} = \frac{V_{bat_{nom}}}{V_{cell_{nom}}} \approx 292 \ [-] \tag{11}$$

$$n_{p,bat} = \frac{E_{bat}}{C_{cell} \cdot V_{bat_{nom}}} \approx 2 \ [-] \tag{12}$$

4 IMC strategies

The operation of battery-hybrid trolleybus may simply be described as a continuous sequence of its operation in trolley mode (i.e. inside the overhead grid) and battery mode (i.e. outside the overhead grid), which is directly influenced by IMC strategy. In reality, the IMC strategy should be adapted according to the requirement of these modes (i.e. driving length and respective time of each mode). The another element which must also be considered is the allowable power of grid during the trolley mode, which in turn dictates the power available for charging besides the normal operation of trolleybus.
To investigate the viability of battery-hybrid trolleybus, a realistic scenario depicting continuous operation is created by combining two measured trips from all the trolleybus lines with the respective highest and second highest energy requirement. Three IMC strategies are developed by considering a allowable grid power of 300 [kW] and SOC operational limit of 40 to 80 %. The three considered IMC strategies are as follows:

- **Ch-1:** continuous charging as quickly as possible with the allowable grid power;
- **Ch-2:** continuous charging as quickly as possible but the allowable grid power is limited to 60 [kW] when the trolleybus is standing still either at the traffic lights or bus stops;
- **Ch-3:** continuous charging but the allowable grid power is adapted such that the trolleybus travels for approx. 10 [km] in the trolley mode while the allowable grid power is limited to 60 [kW] when the trolleybus is standing still either at the traffic lights or bus stops.

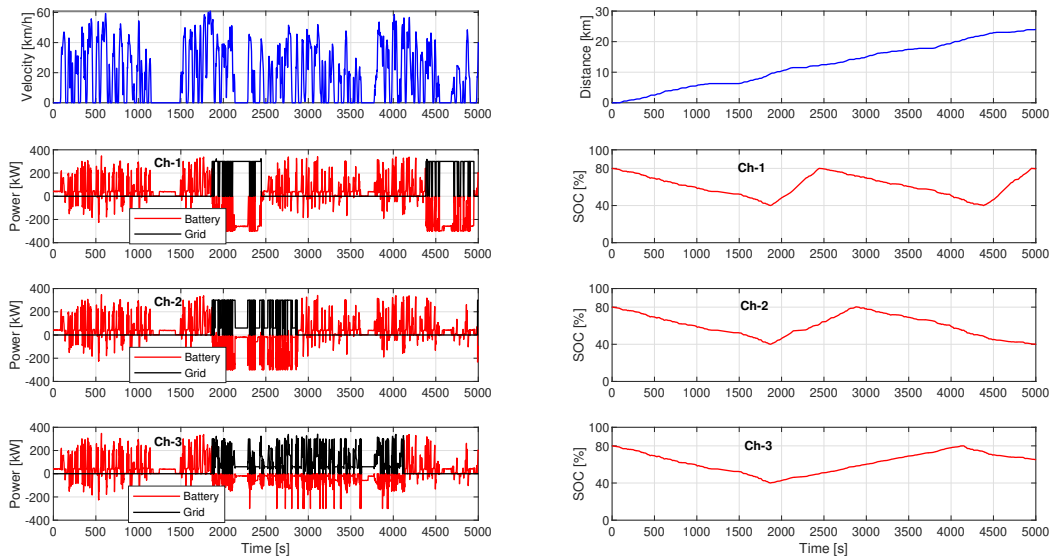

Figure 4: Battery and grid power for the respective IMC strategy

The results of the three IMC strategies are presented in Fig. 4 for first 5000 [s] of the scenario. The difference between the three IMC strategies may be clearly observed from the grid power (black color) and time taken to reach the upper SOC limit in the respective strategy. The total length (or distance travelled) of the simulated scenario is approx. 138.4 [km]. The distance travelled in trolley and battery mode with respect to the IMC strategy is presented in Table 5. The minimum required operation in trolley mode with respect to the IMC strategy may be determined using the time and length ratio. For example, the length ratio of 0.28 in Ch-1 indicates that in order to travel 10 [km] in battery mode, the battery-hybrid trolleybus must travel at least 2.8 [km] in trolley mode prior to battery mode.

Table 5: Summary of IMC strategies for the simulated scenario

IMC strategy	Trolley mode	Battery mode	Total	time ratio	length ratio
Ch-1	30.4 [km]	108 [km]	138.4 [km]	0.26	0.28
Ch-2	39.9 [km]	98.5 [km]	138.4 [km]	0.42	0.41
Ch-3	68.3 [km]	70.1 [km]	138.4 [km]	0.93	0.97

It may also be observed from the time and length ratio of Ch-1 and Ch-2 presented in Table 5 that by limiting the allowable grid power at vehicle stops, leads to increased trolley mode requirement of approx. 1.5 times in case of Ch-2 compared to Ch-1.

5 Discussion and concluding remarks

The traction battery is the key element for realizing the battery-hybrid trolleybuses, which must be capable of fulfilling the energy and power requirement of the trolleybus for the desired driving range. An approach is presented in this work, which can be applied to any of the trolley cities to determine the viability of battery-hybrid trolleybuses and subsequent requirements for the traction battery. However, due to the adapted simplifications and assumptions of the present work, an optimal recommendation with regard to the battery-hybrid trolleybus for the city of Arnhem is limited. These following points addresses these limitations:

- the minimum energy requirement for the traction battery is established using a limited set of measured data. The energy consumption of climate control unit is not critical as it is a controllable quantity when needed. However, the energy consumption of electric motor as described by Equation 5 and 6 depends on multiple variables, which is the essential and more critical part of operation. It is difficult to claim that the present database is able to represent the true dynamics of the respective variables and their combination, especially the external ones such as number of passengers, wind and topography. Therefore, the minimum requirements should be established either based on the large database (at least an year long) or by analysing and quantifying their influence in more detail;

- lithium ion battery with LTO as an anode material is definitely a suitable option due to its high C-rate capability, thermal stability, safety and long life span but the cathode material is also equally relevant which may significantly influence the performance characteristics of the battery as discussed by [9], [12] and subsequently, influences the arrangement and required number of cells in the battery pack. Therefore, the rated energy capacity of the traction battery and required number of cells and their arrangement should be determined after selecting the suitable cathode material;

- the battery model is a simple Rint model which doesn't capture the true transient and dynamic behaviour of the battery due to the absence of RC branch. For such, 1RC or 2RC ECM model is preferred as discussed by [14] - [19]. However, the main limitation of the presented battery model is the unavailability of the thermal model due to which temperature dependencies of the internal resistance and OCV are not incorporated, which may significantly influence the usable capacity of the traction battery and its life span as discussed by [9], [11]. Therefore, it is necessary to include temperature dependencies in the battery model for viability analysis;

- the SOC operational limit is primarily considered to limit the resistive losses and and secondly due to the aforementioned simplifications, which has led to the required energy capacity of 76 [kWh]. However, if the aforementioned arguments are ignored then the traction battery with 40 [kWh] as rated energy capacity and SOC operational limit of 10-90% is also found to be a viable option during the analysis. One of the main and observable difference between the two is the higher discharge and charge rates (approx. twice) for 40 [kWh] battery compared to 76 [kWh] battery, which is due to the number of parallel cells (i.e. 2 in case of 76 [kWh] compared to 1 in 40 [kWh]). Another significant difference is observed in the Ch-1 and Ch-2 IMC strategies. The length and time ratio with respect to 40 [kWh] battery are increased to 0.35 and 0.36, respectively for Ch-1, and 0.65 and 0.59, respectively for Ch-2. It is due to the allowable grid power of 230 [kW] which

is limited by considering the maximum continuous charging current of 360 [A] or C-rate of 6 as described in Table 4.

- the allowable grid power of 300 [kW] considered in the IMC strategies is feasible from the grid perspective. It may also be considered higher (approx. 400 [kW]) as observed from the measured data, which will subsequently reduce the time and length ratio of respective IMC strategy. However, the critical point is the consideration of 60 [kW] as allowable grid power when trolleybus is standing still because it may heat and damage the respective contact point of grid wire. Therefore, this should be further investigated and subsequently, adapted in the respective IMC strategy.

Concluding the limitations of this paper, the next steps in the research are to address the aforementioned points and subsequently, assess the traction battery requirements and IMC strategy. This will lead to an optimal recommendation for the battery-hybrid trolleybus of the city of Arnhem.

Acknowledgments

This research is funded by Interreg e-Bus 2020: In-Motion Charging project. Sincere thanks to Connexxion (Arnhem trolleybus operator) and Kiepe Electric for their cooperation and information.

References

[1] A. M. Danila et.al., *Annual European Union greenhouse gas inventory 1990-2015 and inventory report 2017*, European Environmental Agency (EEA) report (2017).

[2] *Study on network based energy storage systems for Eberswalde*, http://www.trolley-project.eu, accessed on 2019-02-27.

[3] A. Ashrae. *ASHRAE Handbook-HVAC Applications*, American Society of 2011.

[4] C. De Cauwer et.al., *Energy consumption prediction for electric vehicles based on real-world data*, Energies, ISSN 1996-1073, 8.8(2015), 8573-8593.

[5] N. Nitta et.al., *Li-ion battery materials: present and future*, Materials today, 18.5(2015), 252-264.

[6] J. Goodenough et.al., *Challenges for rechargeable Li batteries*, Chemistry of materials, 22.3(2009), 587-603.

[7] R. Zhang et.al., *State of the art of Lithium-ion battery SOC estimation for electrical vehicles*, Energies, 11.7(2018), 1820.

[8] B. G. Pollet et.al., *Current status of hybrid, battery and fuel cell electric vehicles: From electrochemistry to market prospects*, Electrochimica Acta, 84(2012), 235-249.

[9] C. Julien et.al., *Lithium batteries*, In Lithium Batteries, Springer, Cham (2016), 29-68.

[10] E. Vergori et.al., *Battery Modelling and Simulation Using a Programmable Testing Equipment*, Computers, 7.2(2018), 20.

[11] Y. Dongxiang et.al., *Comparing the performances of different energy storage cells for hybrid electric vehicle*, In EVS28 , Kintex, Korea(2015).

[12] K. Ariyoshi et.al., *Conceptual design for 12 V "lead-free" accumulators for automobile and stationary applications*, Journal of Power Sources, 174.2(2007), 1258-1262.

[13] R. F. Nelson, *Power requirements for batteries in hybrid electric vehicles*, Journal of Power Sources, 91.1(2000), 2-26.

[14] X. Lai et.al., *A comparative study of different equivalent circuit models for estimating state-of-charge of lithium ion batteries*, Electrochimica Acta, 259(2018), 566-577.

[15] H. Xiaosong et.al., *A comparative study of equivalent circuit models for Li-ion batteries*, Journal of Power Sources, 198(2012), 359-367.

[16] A. Fotouhi et.al., *A review on electric vehicle battery modelling: From Lithium-ion toward Lithium-Sulphur*, Renewable and Sustainable Energy Reviews, 56(2016), 1008-1021.

[17] H. Hongwen et.al., *Comparison study on the battery models used for the energy management of batteries in electric vehicles*, Energy Conversion and Management, 64(2012), 113-121.

[18] L. Zhang et.al., *Comparative research on RC equivalent circuit models for lithium-ion batteries of electric vehicles*, Applied Sciences, 7.10(2017), 1002.

[19] J. Wehbe et.al., *Battery equivalent circuits and brief summary of components value determination of lithium ion: A review*, In 2015 Third International Conference on Technology Advances in Electrical, Electronics and Computer Engineering (TAEECE), IEEE (2015), 45-49.

[20] *Altairnano 60 Amp Hour Cell*, http://www.altairnano.com/wp-content/uploads/2015/11/60Ah-Cell-Data-Sheet.pdf, accessed on 2019-03-08.

[21] S. Goutam et.al., *Comparative study of surface temperature behaviour of commercial Li-ion pouch cells of different chemistries and capacities by Infrared Thermography*, Energies, ISSN 1996-1073, 8(2015), 8175-8192.

Authors

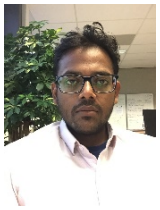

Abhishek Singh Tomar
Vita: 2012: BE in Mechanical Engineering, Manipal University of Technology (India). 2015: MSc in Automotive Systems (HAN). Present work: Researcher at HAN Automotive Research.

Bram P.A. Veenhuizen
Vita: 1984: MSc in Experimental Physics, Free University, Amsterdam. 1988: PhD, University of Amsterdam. Present work: Professor in vehicle mechatronics at HAN.

Lejo Buning
Vita: 1984: BAE in Automotive Engineering, HTS Autotechniek, Apeldoorn. 2012: BBA and 2014: MBA/MSc, Twente School of Management. Present work: Project manager at HAN Automotive Research and PhD candidate at University of Twente.

Ben Pyman
Vita: 2015: BSc in Automotive Engineering, HAN. Present work: Researcher at HAN Automotive Research.